高性能反射防止膜"メソアモルファスコート"用超低屈折率多孔質シリカ薄膜の作製

鈴木涼子

Fabrication of a Porous SiO$_2$ Thin Film with an Ultralow Refractive Index for High Performance Anti-reflective Coatings "Meso Amorphous Coat"[†]

Ryoko SUZUKI

光学機器を製造・販売しているニコンにおいて,反射防止膜は透過率向上や迷光の抑制のために欠かせない重要な技術である.工業的に広く用いられている多層反射防止膜のなかでも,最上層の低屈折率化はその性能向上に最も大きな影響を与える.低屈折率層には空気を含む多孔質構造が求められるが,光の散乱を防ぐためにはその構造は微細なものでなくてはならない.本稿では簡便なゾル-ゲル法を用いた多層反射防止膜の最上層用の低屈折率薄膜の作製について説明する.反応に用いる原料に適切な分子構造の溶媒と高い塩基性を有する塩基触媒を選択することにより,微細な多孔質構造を有する屈折率1.17の多孔質シリカ薄膜を作製することに成功した.膜構造の観察とシミュレーションにより,低散乱および超低屈折率の形成要因を明らかにした.さらに,作製した膜に疎水性官能基を導入することにより空気中の水分の吸着による屈折率変化を低減した.この薄膜は"メソアモルファスコート"の最上層としてカメラレンズに搭載されている.

Anti-reflective coatings are a key technology in Nikon Corporation, which manufactures optical equipment, for improving transmittance and reducing stray light. A lower refractive index of the top layer in the multilayer antireflective coatings, which is widely used in industry, has the greatest effect on improving its performance. The top layer must have a porous structure containing air, but the structure must be fine to prevent light scattering. This paper describes a simple sol-gel method for fabricating a thin film with a low refractive index for the top layer of a multilayer anti-reflective coating. By selecting solvent with appropriate molecular structures and base catalyst with high basicity as raw materials for the reaction, porous SiO$_2$ thin films with a refractive index of 1.17 and a fine porous structure were successfully fabricated. Observation of the film structure and simulation revealed the formation process of low scattering and ultra-low refractive index. Furthermore, by introducing hydrophobic functional groups into the fabricated films, the variation of refractive index due to the adsorption of moisture in the air was reduced. This thin film is applied to camera lenses as the top layer of "Meso Amorphous Coat".

Key words 反射防止膜, 低屈折率膜, 光学薄膜, 多孔質シリカ, ゾル-ゲル法
anti-reflective coating, low refractive index film, optical thin film, porous silica, sol-gel method

1 Introduction

Anti-reflective (AR) coatings are used in various optical products, such as cameras, microscopes, and display panels [1]-[3]. A multilayer AR coating comprises several stacked layers with varying refractive indices [4]. Among these layers, the top layer contributes the most to AR performance. Decreasing the refractive index (n) of the top layer is neces- sary to improve AR performance. MgF$_2$ has the lowest refractive index (n = 1.38) but is not sufficiently low for AR coatings [5].

Most low refractive index materials possess a porous structure. The total refractive index of an AR film can be reduced by forming pores containing air (n = 1) in the film. To date, various porous materials, such as CaF$_2$, MgF$_2$, and Al$_2$O$_3$ have been synthesized [6]–[8]. In particular, SiO$_2$ was

focused on materials for preparing porous structures [9] – [11]. The use of large amount of air to decrease the refractive index of a film tends to cause considerable scattering of light [12], [13]. Moreover, these materials have unstable refractive indices because their pores adsorb moisture from the air easily [14]. To prevent the adsorption of moisture, hydrophilic Si-OH groups of the film surface are often capped. However, the refractive index of the film increases unless the amount of capping agent is controlled [15], [16].

Many studies have reported that a multi-coating of a porous film that contains SiO_2 and whose refractive index is lesser than 1.20 can achieve high transmittance [17], [18]. Therefore, a thin film with n < 1.20 is required for AR coating. However, porous SiO_2 thin films prepared via sol-gel reactions often contain large SiO_2 particles (several tens of nanometers) in their inner structure and exhibit large Rayleigh scattering, which decreases the transmittance of the film [5], [19], [20]. Therefore, a finely structured thin film of porous SiO_2 is required for optical applications. In this study, an easy sol-gel method was used to prepare porous SiO_2 thin films. The obtained porous SiO_2 films exhibited low light scattering and were humidity resistant. In addition, structural analysis and calculations were conducted, and the factors responsible for the low refractive index and scattering were discussed.

2 Experiment

2.1. Materials

Tetramethyl orthosilicate (TMOS; Tokyo Chemical Industry Co., Ltd., Tokyo, Japan) was used as the silica source. 1-Methoxy-2-propanol (PGME; FUJIFILM Wako Pure Chemical Corporation, Osaka, Japan) was used as a solvent. Triethylamine (TEA; Tokyo Chemical Industry Co., Ltd., Tokyo, Japan) was used as the catalyst for the sol-gel reaction. Hexamethyldisilazane (HMDS; Tokyo Chemical Industry Co., Ltd., Tokyo, Japan) was used for the surface treatment of the porous SiO_2 thin films.

2.2. Sample Preparation

The typical preparation methods are described in this section. First, PGME (54.43 g) was poured into a polytetrafluoroethylene (PTFE) bottle. H_2O (1.731 μL), TEA (36.10 μL), and TMOS (7.310 g) were then added into the bottle at a molar ratio of TMOS : H_2O : TEA = $1 : 2 : 0.01$ and stirred for ~27 h at the room temperature. The as-prepared coating liquid containing 4.54 wt% of SiO_2 was filtered using a PTFE filter having a pore size of 5.0 μm and then spin-coated onto

a substrate. The films thus obtained were heated to 160°C for 3 h to obtain a film denoted as $SiO_2\_PGME\_TEA$. After heating, the $SiO_2\_PGME\_TEA$ was treated with HMDS to enhance its hydrophobicity. Subsequently, the film, which was coated on a substrate with 30 mm diameter, was sealed in a closed vessel with HMDS (0.6135 μL) for 24 h at room temperature. Finally, the product was heated at 60 ºC for 0.5 h to form SiO_2_HMDS.

3 Results and Discussions

3.1. Effect of Solvent on SiO_2 Thin Films

The relationship between the sol-gel reaction time and the refractive index of the films was investigated. In addition, the experiment was repeated with different solvents namely, PGME, methanol, 1-propanol, and 1-pentanol, to investigate the effect of a solvent on the relationship. Figure 1 shows the relationship between the sol-gel reaction time and the refractive index of the prepared films. In all cases, the refractive index decreased with reaction time. This behavior was consistent with previously reported results [21]. The behavior is attributed to generating a bulky structure that consists of SiO_2 and enlarges over time in the reaction mixture. The bulkier the SiO_2 structure, the more the number of and larger pores, formed that contain air. Therefore, the refractive index of the thin films decreases over time. The largest decrease in the refractive index was observed when 1-pentanol was used as a solvent. The refractive indices of the thin films prepared using methanol and 1-propanol were almost equal (n ~ 1.20).
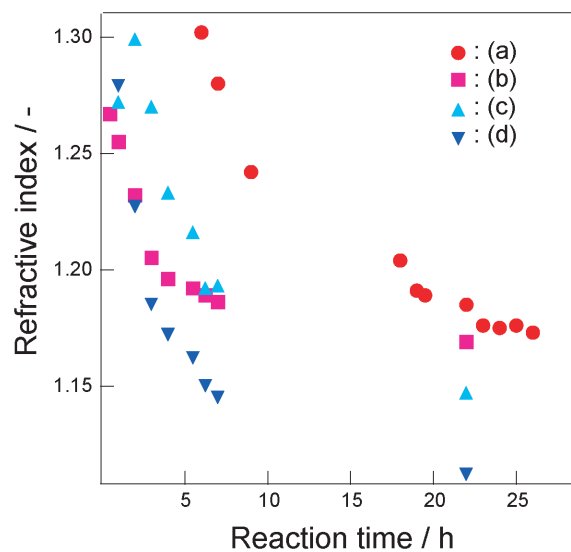

Fig. 1 Relationship between the sol-gel reaction time and the refractive index of thin films prepared with (a) PGME, (b) methanol, (c) 1-propanol, and (d) 1-pentanol as solvents

Figure 2 shows the relationship between refractive index of the film prepared from the coating liquid reacted for an arbitrary time and transmittance at 350 nm of the same coating liquid for different solvents. In all cases, the transmittance and refractive index decreased with reaction time simultaneously. As shown in Fig. 1, SiO_2 structures grew and aggregated in coating liquid during the sol-gel reaction, which increased the porosity of the SiO_2 thin films. Figure 2 provides data to consider how SiO_2 fine structure can be formed without particle growth and aggregation, increasing scattering and decreases transmittance. The transmittance corresponding to PGME was higher than that corresponding to methanol and 1-propanol when the refractive indices of the thin films were almost the same; for example, the refractive index was approximately 1.20. The reaction mixture containing 1-pentanol exhibits the highest transmittance. These results indicate that finely structured SiO_2 was formed when PGME and 1-pentanol were used as solvents.
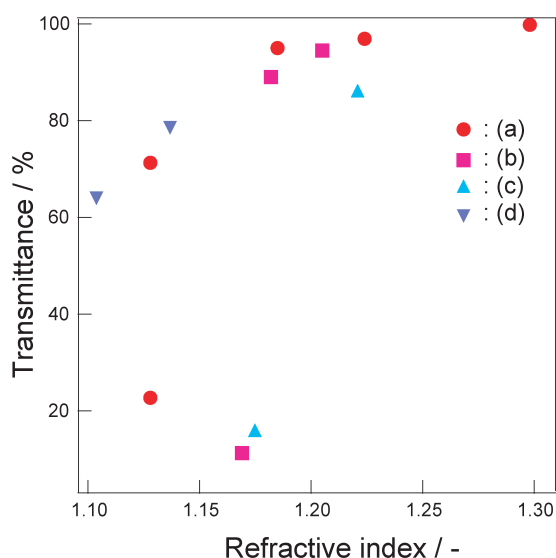

Fig. 2 Relationship between refractive index of the thin film and the corresponding transmittance at 350 nm of the same coating liquid prepared using (a) PGME, (b) methanol, (c) 1-propanol, and (d) 1-pentanol

The results showed transesterification occurred between the methoxy group of TMOS and the solvent during the sol-gel reaction. The reactivity of silanes that underwent transesterification was lower than that of TMOS, possibly because silanes contain a bulkier alkoxy group than TMOS. The bulky alkoxy group on the surface of the SiO_2 structure prevented the aggregation of the SiO_2 particles. The transesterification reaction also prevented the growth and aggregation of SiO_2 structures. In addition, PGME is considered a suitable solvent for controlling the refractive index of AR coatings because it tends to reduce the refractive index near

1.20 gradually.

Figure 3 shows the photographs and optical microscopic images of the thin films prepared in this study. As shown in Fig. 3a-b, radial striations can be observed in the SiO_2 thin film surface prepared using methanol. In contrast, thin films prepared using 1-propanol (Fig. 3c-d), 1-pentanol (Fig. 3e-f), and PGME (Fig. 3g-h) exhibit smooth surfaces.
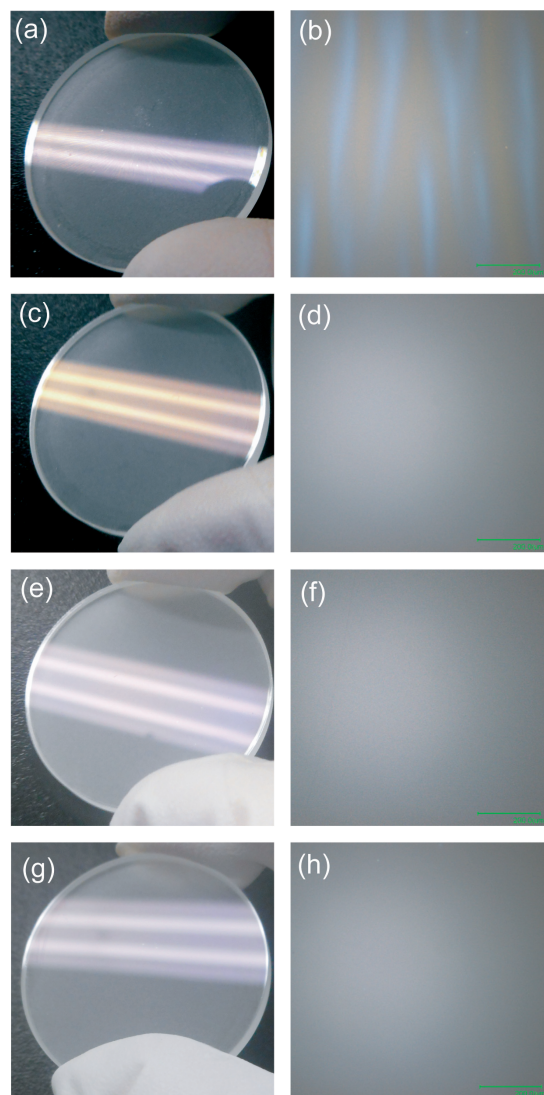

Fig. 3 Appearance of a thin film prepared using a coating liquid containing (a) methanol, (c) 1-propanol, (e) 1-pentanol, and (g) PGME; (b), (d), (f), and (h) represent the corresponding optical microscopic images. (Scale bar in b, d, f, and h represents 200 μm.)

From the above results, PGME can be considered a suitable solvent for fabricating porous silica thin films as AR coating from view points of control of refractive index and appearance.

3.2. Effect of the Base on the Structure of Porous SiO_2 Thin Films

To investigate the effect of the base on the structure of SiO_2 thin films, SiO_2 thin films were prepared using NH_3,

propylamine (PA), and diethylamino (DEA) in place of TEA in the original preparation method. In each experiment, the refractive index of the thin films was adjusted to n = 1.17 by controlling the reaction time.

Figure 4 shows the cross-sectional SEM images of the thin films. A SiO_2 framework comprising small connected particles was observed in all porous SiO_2 thin films. In Fig. 4, the diameter of a SiO_2 primary particle was considered corresponding to the thickness of the framework. Therefore, the SiO_2 primary particle diameter was measured at four points and averaged in each SEM image. SiO_2_PGME_NH_3 (Fig. 4a) and SiO_2_PGME_PA (Fig. 4b) possessed thick frameworks. The second thinnest and thinnest frameworks were observed in SiO_2_PGME_DEA (Fig. 4c) and SiO_2_PGME_TEA (Fig. 4d), respectively. The thicknesses of the SiO_2_PGME_NH_3, SiO_2_PGME_PA, SiO_2_PGME_DEA, and SiO_2_PGME_TEA frameworks, measured using their SEM images, were 15.8 nm, 15.3 nm, 11.0 nm, and 9.8 nm, respectively.
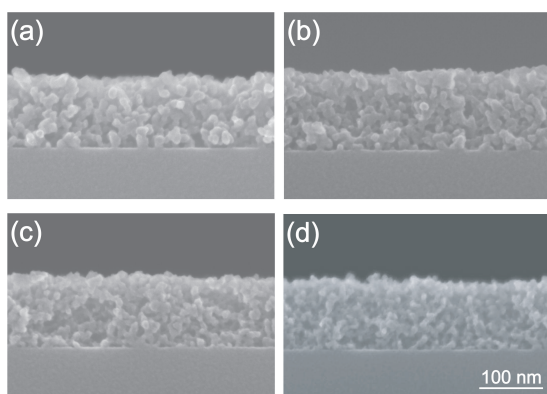

Fig. 4　Cross-sectional SEM images of (a) SiO_2_PGME_NH_3, (b) SiO_2_PGME_PA, (c) SiO_2_PGME_DEA, and (d) SiO_2_PGME_TEA

Table 1 shows the amount of scattered light at 350 nm by thin films. The amount of light scattered by SiO_2_PGME_PA was the highest, whereas that scattered by SiO_2_PGME_TEA was the smallest.

Figure 5 shows the viscosity of the reaction mixture to reaction time. The viscosity increased with reaction time for samples prepared using PA, DEA, and TEA catalysts. Nota-

Table 1　Amount of scattered light at 350 nm by the porous SiO_2 thin films

	Amount of scattering at 350 nm/ppm
SiO_2_PGME_NH_3	248
SiO_2_PGME_PA	388
SiO_2_PGME_DEA	265
SiO_2_PGME_TEA	204

bly, the maximum increase in viscosity is observed for TEA. The type of basic catalyst affected the formation of SiO_2 because of the inductive effect, steric hindrance of the catalysts and solvent [22]. The pKa values of NH_3, propylamine, diethylamine and triethylamine in water are 9.21, 10.53, 10.98 and 10.65, respectively [23]. It means that basicity decreases in the order diethylamine > triethylamine > propylamine > NH_3. However, the pKa values listed here are those in water, which have been widely reported, and these values vary with the solvent. It has been reported that tertiary amines may have a higher pKa than secondary amines in organic solvents [24]. This is owing to the stability of the generated cationic species in the solvent and other factors. Therefore, it must be noted that the reaction of this study was carried out in an organic solvent, mainly PGME. Furthermore, the composition of solvent was changed with the progress of reaction owing to methanol produced by hydrolysis. Therefore, discussing the reactivity of the base from the pKa value of a particular solvent is difficult. However, TEA has the highest reactivity in PGME than other bases. This may be because TEA has three alkyl chains, which are electron-donating groups, and the $NH(C_2H_5)^{3+}$ generated from TEA has stability in organic solvents owing to its three alkyl chains. SEM images and viscosity measurements showed that small SiO_2 nanoparticles were simultaneously generated and interconnected when TEA was used as a basic catalyst.

These results indicate that the structure of the porous SiO_2 thin films differed depending on the organic base used. In particular, a fine-structured low-scattering film was obtained using a highly basic catalyst (TEA). However, gelation did not
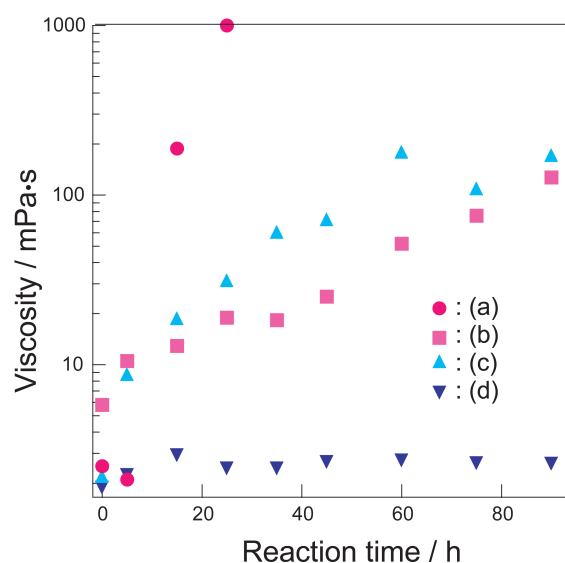

Fig. 5　Viscosity of the reaction mixture containing (a) TEA, (b) DEA, (c) PA, and (d) NH_3 as the catalyst to reaction time

proceed when NH_3 was used as a basic catalyst. The refractive index of the thin film could be decreased by interlinking small SiO_2 nanoparticles using TEA and by growing SiO_2 nanoparticles using NH_3. In conclusion, TEA is a suitable catalyst for synthesizing porous SiO_2 thin films for AR coating.

3.3. Inner and Surface Structure of a Thin Film

The Structural characteristics of SiO_2_PGME_TEA (n = 1.17) were investigated. Figure 6 shows the pore distribution measured via positron annihilation spectroscopy. Two peaks were observed at 0.48 nm and 2.4 nm. The peak at 0.48 nm could be attributed to the gap in the siloxane framework [25] and that at 2.4 nm could be ascribed to the presence of pores in SiO_2 films.
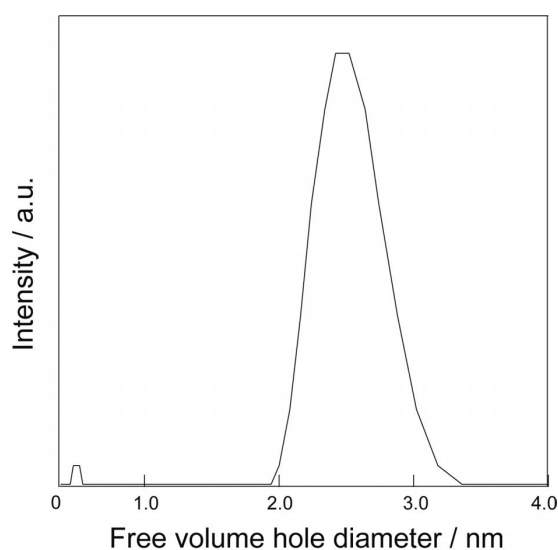
Fig. 6 Pore size distribution of SiO_2_PGME_TEA (n = 1.17) measured using positron annihilation spectroscopy

Figure 7 shows a 3D-TEM image of SiO_2_PGME_TEA. The colored areas represent pores that were detected by image analysis. Several pores were distributed inside the film. Image analysis also revealed the pore distribution, which showed that the pore diameter was in the range of 2–3 nm. This is consistent with the results induced via positron annihilation spectroscopy. Additionally, porosity was calculated to be 65 vol % via image analysis. Considering that the refractive index calculated from the reflectance measurement was n = 1.17, the porosity of the film was calculated from the Lorentz–Lorentz formula using the refractive index of SiO_2 and air and their volume fractions [26]. The porosity calculated using the refractive index was 62.2 vol %. This result indicates that a 3D-TEM structural analysis was appropriate. Therefore, SiO_2_PGME_TEA was confirmed to possess abundant pores of diameter 2–3 nm and a high porosity of over 60 vol%. This high porosity was attributed to

the bulky colloidal SiO_2 structure grown in the coating liquid. If SiO_2 in the coating liquid were mono-dispersed spherical particles, the porosity of porous SiO_2 thin films would be 49.4 vol%, as calculated using Structure of NAno Particles (SNAP) simulation [27], [28]. This shows that the SiO_2 in the coating liquid possessed a bulky structure formed by connecting small SiO_2 nanoparticles. Because bulky SiO_2 structures could not be densely packed like mono-dispersed spherical nanoparticles, they formed a highly porous SiO_2 thin film.
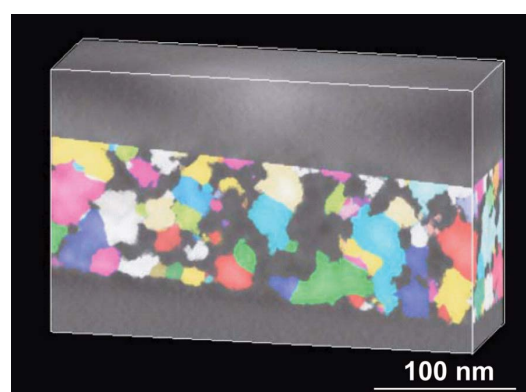

Fig. 7 3D-TEM image of SiO_2_PGME_TEA
The refractive indices of the films were adjusted to n = 1.17. Colored areas were detected pores using image analysis.

The size of the pores in SiO_2_PGME_TEA (2–3 nm) was smaller than the wavelength of visible light, indicating that SiO_2_PGME_TEA can exhibit a low scattering of light [29].

3.4. Enhanced Hydrophobicity of SiO_2_PGME_TEA

The adsorption of moisture from air into porous SiO_2 was reported to increase the refractive index [14]. When porous SiO_2 is used for AR coating, increasing the refractive index affects the optical properties. Therefore, the Si-OH groups in SiO_2_PGME_TEA should be capped by hydrophobic groups. HMDS was used for capping the Si-OH groups because it is commonly used for hydrophobization [30].

In the infrared reflection-absorption spectra (IR-RAS) (Fig. 8) of SiO_2_PGME_TEA and SiO_2_HMDS, an adsorption band at 1250 cm^{-1} was observed in only SiO_2_HMDS, which was assigned to v(Si-C) [31]. It showed that HMDS was introduced into SiO_2_PGME_TEA.

In addition, the contact angles of SiO_2_PGEM_TEA and SiO_2_HMDS were measured to be 8.7° and 65°, respectively (Fig. 9). This indicated that SiO_2_PGEM_TEA possessed a hydrophilic surface, whereas SiO_2_HMDS possessed a hydrophobic surface. These results revealed that HMDS successfully capped the Si-OH group and increased the
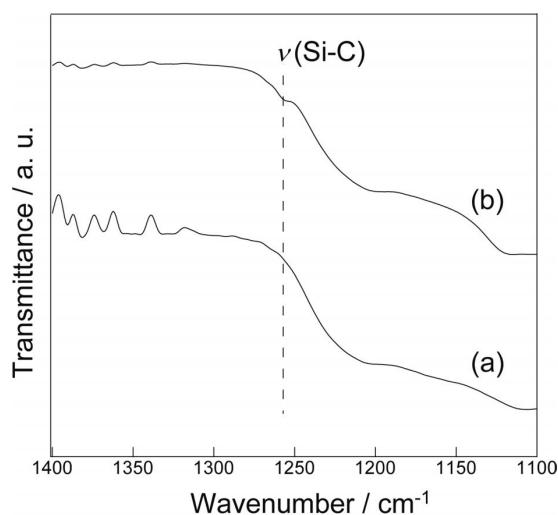
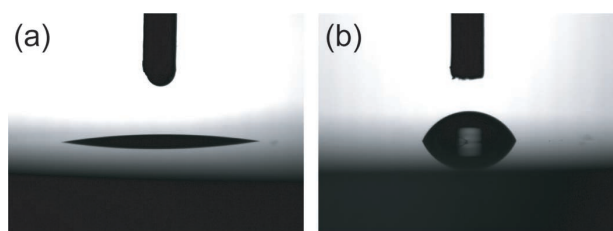Fig. 8　IR-RAS spectra of SiO$_2$_PGME_TEA (a) before and (b) after HMDS treatment

Fig. 9　Contact angle measurement of SiO$_2$_PGME_TEA (a) before and (b) after HMDS treatment

hydrophobicity of SiO$_2$_PGME_TEA.

The refractive indices of SiO$_2$_PGME_TEA and SiO$_2$_HMDS are listed in Table 2. The refractive index of SiO$_2$_HMDS was higher than that of SiO$_2$_PGME_TEA. It probably indicated that HMDS was introduced into the pores of SiO$_2$_PGME_TEA. Moreover, the changes in refractive indices after keeping the films at 24℃ and 35% relative humidity for 7 d were compared. The increase in the refractive index of SiO$_2$_HMDS was smaller than that of SiO$_2$_PGME_TEA for 7 d.

Table 2　Refractive indices of SiO$_2$_PGME_TEA and SiO$_2$_HMDS on 0, and 7 d

	n on day 0/ -	n on day 7/ -	Increase in n after 7 d/ -
SiO$_2$_PGME_TEA	1.170	1.212	0.042
SiO$_2$_HMDS	1.197	1.209	0.012

Hence, the HMDS treatment prevented an increase in the refractive index of the porous SiO$_2$ thin films via the capping of the Si-OH groups.

4　Conclusion

Porous SiO$_2$ thin films having low refractive indices were successfully prepared via a simple sol-gel method. The choice of solvent and basic catalyst is a key factor for controlling the reactivity of the coating liquid and forming a smooth film that exhibits low scattering. The porous SiO$_2$ thin film fabricated in this study could be used as a broadband AR coating with stacked undercoating and as a lens and sensor in various optical devices.

References

[1] H. G. Shanbhogue, C. L. Nagendra, M. N. Annapurna, S. A. Kumar, and G. K. M. Thutupalli, "Multilayer antireflection coatings for the visible and near-infrared regions," *Appl. Opt.*, vol. 36, pp. 6339–6351, 1997.

[2] X. Li, J. Gao, L. Xue, and Y. Han, "Porous polymer films with gradient-refractive-index structure for broadband and omnidirectional antireflection coatings," *Adv. Funct. Mater.*, vol. 20, pp. 259–265, 2010.

[3] D. Chen, "Anti-reflection (AR) coatings made by sol-gel processes: a review," *Solar Sol. Energy Mater. Sol. Cells*, vol. 68, pp. 313–336, 2001.

[4] X. Sun, J. Tu, L. Li, W. Zhang, and K. Hu, "Preparation of wide-angle and abrasion-resistant multi-layer antireflective coatings by MgF$_2$ and SiO$_2$ mixed sol," *Colloids Surf.*, *A*, vol. 602, 125106, 2020.

[5] X. Zhang, P. Lan, Y. Lu, J. Li, H. Xu, J. Zhang, Y. P. Lee, J. Y. Rhee, K. L. Choy, and W. Song, "Multifunctional antireflection coatings based on novel hollow silica–silica nanocomposites," *ACS Appl. Mater. Interfaces*, vol. 6, pp. 1415–1423, 2014.

[6] I. M. Thomas, "Porous fluoride antireflective coatings," *Appl. Opt.*, vol. 27, pp. 3356–3358, 1988.

[7] S. Fujihara, Y. Kadota, and T. Kimura, "Role of organic additives in the sol-gel synthesis of porous CaF$_2$ antireflective coatings," *J. Sol-Gel Sci. Tech.*, vol. 24, pp. 147–154, 2002.

[8] N. Yamaguchi, K. Tadanaga, A. Matsuda, T. Minami, and M. Tatsumisago, "Antireflective properties of flowerlike alumina thin films on soda-lime silica glass substrates prepared by the sol-gel method with hot water treatment," *Thin Solid Films*, vol. 515, pp. 3914–3917, 2007.

[9] I. M. Thomas, "High laser damage threshold porous silica antireflective coating," *Appl. Opt.*, vol. 25, pp. 1481–1483, 1986.

[10] J. Moghal, J. Kobler, J. Sauer, J. Best, M. Gardener, A. A. R. Watt, and G. Wakefield, "High-performance, single-layer antireflective optical coatings comprising mesoporous silica nanoparticles," *ACS Appl. Mater. Interfaces*, vol. 4, pp.

854–859, 2012.

[11] A. Vincent, S. Babu, E. Brinley, A. Karakoti, S. Deshpande, and S. Seal, "Role of catalyst on refractive index tunability of porous silica antireflective coatings by sol-gel technique," *J. Phys. Chem. C*, vol. 111, pp. 8291–8298, 2007.

[12] M. P. J. Peeters and M. R. Bohmer, "Optical application of (pigmented) sol-gel coatings," *J. Sol-Gel Sci. Technol.*, vol. 26, pp. 57–62, 2003.

[13] C. Murray, C. Flannery, I. Streiter, S. E. Schulz, M. R. Baklanov, K. P. Mogilnikov, C. Himcinschi, M. Friedrich, D. R. T. Zahn, and T. Gessner, "Comparison of techniques to characterise the density, porosity and elastic modulus of porous low-*k* SiO$_2$ xerogel films," *Microelectron. Eng.*, vol. 60, pp. 133–141, 2002.

[14] Z. Wang and Z. Gu, "Optical humidity-sensitive mechanism based on refractive index variation," *Chin. Opt. Lett.*, vol. 7, pp. 756–759, 2009.

[15] W. Dou, P. Wang, D. Zhang, and J. Yu, "An efficient way to prepare hydrophobic antireflective SiO$_2$ film by sol-gel method," *Mater. Lett.*, vol. 167, pp. 69–72, 2016.

[16] S. Zhang, P. Xiao, P. Wang, J. Luo, and B. Jiang, "Spherical-chain silica with super-hydrophobic surface and ultra-low refractive index for multi-functional broadband antireflective coatings," *Sol. Energy*, vol. 207, pp. 1222–1230, 2020.

[17] X. Huang, Y. Yuan, S. Liu, L. Zhang, and R. Hong, "Preparation of hydrophobic broadband antireflective SiO$_2$ coating on flexible poly (methyl methacrylate) substrates," *Colloid Surf. A-Physicochem. Eng. Asp.*, vol. 538, pp. 519–525, 2018.

[18] H. T. Hsu, C. Y. Ting, C. Y. Mou, and B. Z. Wan, "Nanoporous SiO$_2$ films prepared by surfactant templating method - a novel antireflective coating technology," *Stud. Surf. Sci. Catal.*, vol. 146, pp. 539–542, 2003.

[19] H. Ren, J. Zhu, Y. Bi, Y. Xu, and L. Zhang, "Assembly of methylated hollow silica nanospheres toward humidity-resistant antireflective porous films with ultralow refractive indices," *J. Porous Mater.*, vol. 25, pp. 55–62, 2018.

[20] J. H. Rouse and G. S. Ferguson, "Preparation of thin silica films with controlled thickness and tunable refractive index," *J. Am. Chem. Soc.*, vol. 125, pp. 15529–15536, 2003.

[21] K. Makita, Y. Akamatsu, and A. Takamatsu, "Sol-gel preparation of silica films with controlled surface morphology and their application to a low reflective glass," *J. Sol-Gel Sci. Technol.*, vol. 14, pp. 175–186, 1999.

[22] R. D. Hancock, B. S. Nakani, and F. Marsicano, "Relationship between Lewis acid-base behavior in the gas phase and in aqueous solution. 1. role of inductive, polarizability, and steric effects in amine ligands," *Inorg. Chem.*, vol. 22, pp. 2531–2535, 1983.

[23] J. F. Coetzee and G. R. Padmanabhan, "Properties of bases in acetonitrile as solvent. IV. proton acceptor power and homoconjugation of mono- and diamines," *J. Am. Chem. Soc.*, vol. 87, pp. 5005–5010, 1965.

[24] M. D. Cantu, S. Hillebranda, and E. Carrilho, "Determination of the dissociation constants (pK_a) of secondary and tertiary amines in organic media by capillary electrophoresis and their role in the electrophoretic mobility order inversion," *J. Chromatogr. A*, vol. 1068, pp. 99–105, 2005.

[25] M. Misheva, N. Djourelov, F. M. A. Margaca, and I. M. M. Salvado, "Positronium study of porous structure of sol-gel prepared SiO$_2$: influence of pH," *J. Non-Cryst. Solids*, vol. 279, pp. 196–203, 2001.

[26] P. Falcaro, D. Grosso, H. Amenitsch, and P. Innocenzi, "Silica orthorhombic mesostructured films with low refractive index and high thermal stability," *J. Phys. Chem. B*, vol. 108, pp. 10942–10948, 2004.

[27] K. Hasegawa, A. Nasu, and M. Fuita, "Behavior analysis of coating layer particles in cosmetic materials during drying by observation and computational simulation," *Mathematical Monographs*, vol. 9, pp. 75–88, 2016.

[28] M. Fujita and Y. Yamaguchi, "Development of three-dimensional structure formation simulator of colloidal nanoparticles during drying," *J. Chem. Eng. Jpn.*, vol. 39, pp. 83–89, 2006.

[29] P. K. Jain, K. S. Lee, I. H. El-Sayed, and M. A. El-Sayed, "Calculated absorption and scattering properties of gold nanoparticles of different size, shape, and composition: applications in biological imaging and biomedicine," *J. Phys. Chem. B*, vol. 110, pp. 7238–7248, 2006.

[30] O. Nalamasu, M. Cheng, A. G. Timko, V. Pol, E. Reichmanis, and L. F. Thompson, "An overview of resist processing for deep-UV lithography," *J. Photopolym. Sci. Technol.*, vol. 4, pp. 299–318, 1991.

[31] T. Hirotsu and C. Tagaki, "Plasma copolymer membranes of acrylic acid and the adsorption of lysozyme on the surface," *Thin Solid Films*, vol. 457, pp. 20–25, 2004.

鈴木涼子　Ryoko SUZUKI
先進技術開発本部 材料・要素技術研究所
Materials & Advanced Research Laboratory
Advanced Technology Research & Development Division

鈴木涼子
Ryoko SUZUKI